International Conference on Space Optics—ICSO 2008

Toulouse, France

14–17 October 2008

Edited by Josiane Costeraste, Errico Armandillo, and Nikos Karafolas

JWST-MIRI spectrometer main optics design and main results

Ramón Navarro

Ton Schoenmaker

Gabby Kroes

Ad Oudenhuysen

et al.

esa icso proceedings cnes

International Conference on Space Optics — ICSO 2008, edited by Josiane Costeraste, Errico Armandillo, Nikos Karafolas, Proc. of SPIE Vol. 10566, 105662C · © 2008 ESA and CNES
CCC code: 0277-786X/17/$18 · doi: 10.1117/12.2308224

JWST-MIRI SPECTROMETER MAIN OPTICS DESIGN AND MAIT RESULTS.

Ramón Navarro, Ton Schoenmaker, Gabby Kroes, Ad Oudenhuysen, Rieks Jager, Lars Venema

NOVA-ASTRON, Oude Hoogeveensedijk 4, 7991 PD Dwingeloo, The Netherlands, E-mail: pr@astron.nl

ABSTRACT

MIRI ('Mid InfraRed Instrument') is the combined imager and integral field spectrometer for the 5-29 micron wavelength range under development for the James Webb Space Telescope JWST. The flight acceptance tests of the Spectrometer Main Optics flight models (SMO), part of the MIRI spectrometer, are completed in the summer of 2008 and the system is delivered to the MIRI-JWST consortium.

The two SMO arms contain 14 mirrors and form the MIRI optical system together with 12 selectable gratings on grating wheels. The entire system operates at a temperature of 7 Kelvin and is designed on the basis of a 'no adjustments' philosophy. This means that the optical alignment precision depends strongly on the design, tolerance analysis and detailed knowledge of the manufacturing process. Because in principle no corrections are needed after assembly, continuous tracking of the alignment performance during the design and manufacturing phases is important.

The flight hardware is inspected with respect to performance parameters like alignment and image quality. The stability of these parameters is investigated after exposure to various vibration levels and successive cryogenic cool downs. This paper describes the philosophy behind the acceptance tests, the chosen test strategy and reports the results of these tests. In addition the paper covers the design of the optical test setup, focusing on the simulation of the optical interfaces of the SMO. Also the relation to the SMO qualification and verification program is addressed.

1. INTRODUCTION

The Mid-Infrared Instrument (MIRI) [4] for the James Webb Space Telescope (JWST) is a thermal-infrared imager and spectrometer currently being developed by an international consortium that consists of over 20 partners. The medium resolution integral field spectrometer (R = 1000 - 3000) will operate in mid-infrared wavelengths with four wavelength channels that cover the full range of 5 – 29 μm, and fields of view from 3x3 arcsec (5 μm) to 7x7 arcsec (29 μm). The medium resolution spectrometer is divided into the Spectrometer Pre Optics (SPO) and the Spectrometer Main Optics (SMO) subsystems [1] & [3]. The SPO contains the waveband separation dichroics, anamorphic optics, the integral field units (IFU) and the dispersing elements (reflection gratings). The SMO contains the collimators and the cameras which image the spectra of all IFU output slices onto the two 1024x1024 pixels Focal Plane Arrays (FPA).

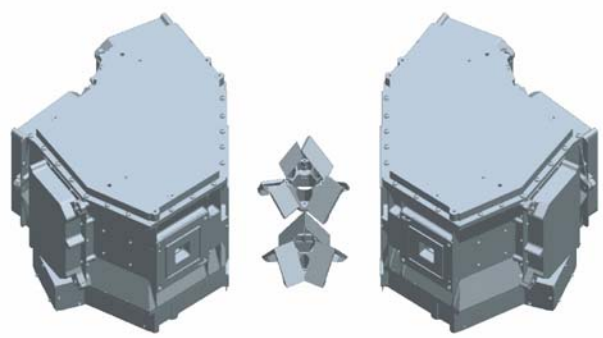

Fig. 1. The SMO design (SW left and LW right) with the gratings (part of the SPO, shown in the center).

1.1 ALIGNMENT & TOLERANCING

The development of an optical instrument like MIRI starts with the translation of the science requirements into a basic optical design. Detailed optical modeling eventually results in a full description of the optical system, i.e. the parameters of the optical surfaces, their precise locations, the image quality for all wavelengths and field positions and a full description of the optical beams geometry. This extensive set of parameters is then used as first input for the mechanical design. Interaction between optical and mechanical design results in optimization of both. The optical model can thus be regarded as the skeleton of the instrument. The mechanical model is wrapped around this skeleton in order to create a physical instrument with actual optics and support structures. By means of 3D mechanical modeling, supported by mechanical structure analysis, the real opto-mechanical system is created. In order to guide the design, the rather complex description of optical performance is condensed into a set of requirements on the image quality and position; both focus and lateral position, of the final spectra. Through an optical sensitivity analysis the alignment

requirements for all optics are translated into surface form and position tolerances (6 degrees of freedom) of the individual optical elements. The overall alignment performance clearly depends strongly on the properties of both the optical and the mechanical design, but in addition there are many 'external' issues that should be taken into account, like launch, transition to zero gravity, ageing, cool-down.

1.2 ALIGNMENT PHILOSOPHY

Contrary to the traditional practice of alignment during assembly, for the SMO an alignment philosophy is adopted that is based on manufacturing precision. This method has already been used successful with similar ground based infrared instrumentation like MIDI and VISIR [1]. This "no adjustments strategy" has a large impact on the whole instrument development process. Big advantages can be achieved not only in the final instrument performance, but also in programmatic issues like schedule and costs. An essential part of the optical design is the optical tolerance analysis, which provides error budgets for all optical elements of the spectrometer. First of all separate allocations of the subsystem error budgets are determined for SMO and SPO. Through the optical sensitivity analysis these error allocations are then narrowed down to budgets for surface form and position at component level and these are input for the mechanical design.

2. SMO IMAGE QUALITY AND ALIGNMENT SENSITIVITY

In principle all the single errors on each individual optical element contribute to the final image position and quality. The image quality is specified by means of optical wavefront errors. Image position errors are separated into lateral 'bore sight' errors and focus errors.

Image quality

The final image quality is mainly influenced by the accuracy of the final surface form of each individual piece of optics. This optical surface form will not only be achieved by the precision of manufacturing but also by the opto-mechanical design choices like shape of mirror substrate, type of lightweighting and - most importantly - the way of mounting of the optics. The effects on the overall SMO image quality of final positioning errors of the optical surfaces are very small and insignificant with respect to the effects through surface form. This has the important advantage that in our case the shape and positioning errors are essentially decoupled.

Image position

We consider the two components of image position errors separately. The focus errors are the axial displacements of the final image with respect to the optimum position; the bore sight errors cover the lateral displacements in the detector image plane.

Image focus

The SMO optical design is special in two ways. Firstly, since there are four wavelengths channels but only two detectors, two images (sets of spectra) are projected onto one detector while the corresponding optical beams share only part of the optics. Secondly, the fast output F-ratios ask for very precise focusing of the detector. As a consequence of these two facts, two exceptions to the "no adjustment" design philosophy were made:

a) in order to ensure alignment of the foci of the two sets of spectra per detector to a common focal plane a shim in one of the beams (at the M1 mounting) is foreseen which allows differential focus adjustment after final assembly;

b) fine-adjustment of the final detector focus position is possible by post-machining of a dedicated shim in the detector mounting.

Image bore sight

The image bore sight error is the lateral displacement of the image on the detector with respect to the nominal image position. The final position of the image is mainly influenced by the positions (mostly the tilts) of the individual optical surfaces. The displacement sensitivity (displacement amplitude per component translation/rotation) varies strongly per optical element. In the SMO the bore sight errors are far more sensitive to alignment problems than the wavefront errors (image quality). To determine the effects of mechanical misalignments the bore sight errors are used to qualify the mechanical design. The allowable bore sight errors are derived from the optical sensitivity analysis which gives the effect of individual component misalignment (in all six degrees of freedom) on the final image position.

2.1 MECHANICAL DESIGN

Early interaction between the optical and mechanical design, as well as high level design choices, resulted in a very specific lay-out (figure 1) consisting of two mirrored modules and two separate grating wheels (located within the SPO). This allows identical designs for the mirrors in the two modules and mirror image designs for the structures. Because only one module needs to be fully designed and tested and the other module follows with relatively little effort; important advantages are reached with respect to design effort, cost and schedule.

Mounting principles, mirror design and the way of manufacturing are some of the main contributors to the final shape and orientation accuracy of the optical

surfaces. In order to find the best design principles and manufacturing methods a thorough concept study is performed. The details of that study are outside the scope of this paper, but have been described already in [2]. Every separately manufactured interface influences the total error of an individual component. This concerns not only the interfaces in the final instrument, but also intermediate interfaces e.g. with manufacturing tooling.

By design the number of interfaces within the instrument is kept as small as possible by creating all final interfaces of the structure in one single fixture. Extra care is taken to create maximum accessibility to these interface surfaces by locating them on the outside of the structure.

3. ALIGNMENT VERIFICATION & STABILITY

The design effort as discussed in section 2 results in a complete alignment budget. This budget includes estimates of the alignment after assembly, but also includes estimated pixel shifts due to the environment the SMO is subjected to during its lifetime. In this way the budget provides confidence that the design is feasible with respect to the alignment requirements even before verification activities started. This budget is created with help of an end-to end analysis.

End to end analysis
The overall alignment performance depends strongly on the properties of both the optical and the mechanical design. An integrated opto-mechanical analysis, or end-to-end analysis, is the best method of continuous alignment monitoring.

Measurements & Tests
This alignment budget has been and still is almost continuously verified from the moment the design was started until the last alignment measurement of the final hardware. During the early design stages this is done by means of different kinds of analysis, later it is supported by actual measurements, when physical components become available. When the mechanical design of the SMO was evolving enough information became available to start manufacturing representative models. With help of these models measurements and tests can be executed to verify the assumed environmental contributions in the alignment budget. A more thorough discussion on the SMO verification philosophy can be found in [7]. First a so called qualification model (QM) is manufactured that is representative to the strength and stiffness of the design. Shortly later a verification model (VM) is built that is also representative to the optical parameters. Finally the flight models (FM) are produced.

Vibration Test
Vibration tests are performed to test the design against the mechanical loads during launch. Static loads are tested with a sine test and dynamical loads are tested with a random vibration test. The sine test is representative as a static load tests since the mechanical properties (SMO first fundamental frequency > sine test frequency range) make the SMO behave only statically during the sine test.

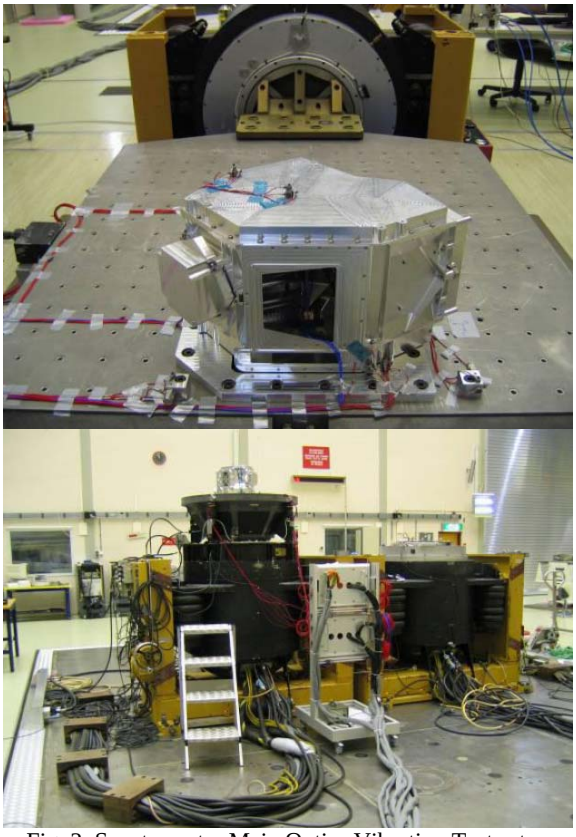

Fig. 2. Spectrometer Main Optics Vibration Test setup

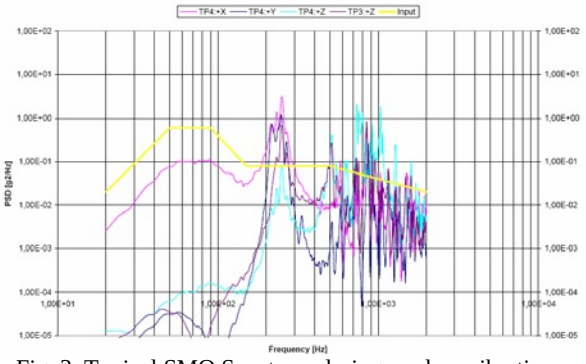

Fig. 3. Typical SMO Spectrum during random vibration.

Gravity release Test
In outer space the effect of gravity is cancelled, in contrast with the measurement conditions on earth. To assess this effect, alignment is measured with different gravity vector orientations. Because all flexed mirrors

have the same orientation with respect to the gravity vector, two orientations are sufficient to assess any gravity release effects (+1 g and -1 g), where the measured quantity is 2 times the expected quantity due to gravity release.

Thermal Vacuum Cycling Test (TVC)
Although the performance at cryogenic temperatures is not verified, it was deemed necessary to check the performance stability of the SMO after successive cycles to cryogenic temperatures. Therefore the SMO is cooled to temperatures below 77 K for 10 times. The lower qualification temperature differs significantly from the SMO operational temperature of 7 K. This limits the cost of TVC tests with a great amount, but with keeping the test significant enough. Since the SMO is an all Al-6061 structure, 99% of the shrinkage has taken place when cooled to 77 K.

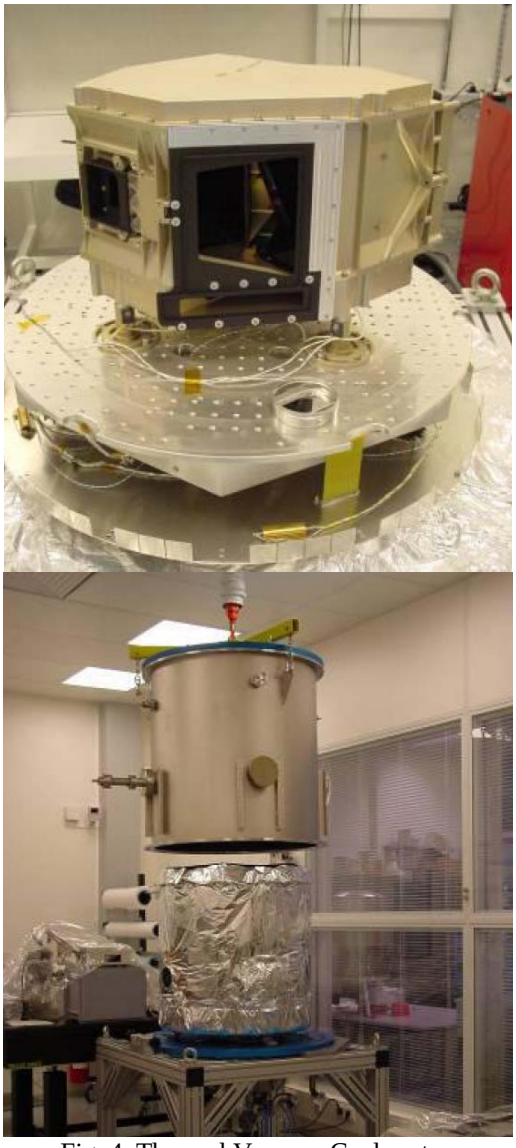

Fig. 4. Thermal Vacuum Cycle setup

4. MEASUREMENT SETUP AND RESULTS

4.1 IMAGE FOCUS
For all channels of the SW and LW arm, the centre and edges of the slits are mimicked by three laser spots. These Slit Simulator Modules (SSM) direct a telecentric beam into the SMO. After reflection off the collimator mirrors, the beams of each channel coincide on the Grating Simulation Mirrors (GSM). The tilts of the GSMs are chosen to simulate the wavelength range for each cannel: short, mid and long wavelength.

The collimated beams reflected off the GSMs are imaged by mirrors M1-1/M1-2, M2 and M3 onto the detector. The three field positions of the SSM and the three wavelengths simulated by tilting the GSM provide for each channel nine spots on the detector. Figure 6 shows the position of the spots.

To determine best focus of an image spot, a piece of ground glass is moved through focus using a micrometer screw. The Z-position of the ground glass is measured and a microscope camera is kept focused on the ground glass by moving the system simultaneously with the ground glass. Pictures are taken at 11 ground glass positions around the estimated best focus (total range is 0.300 mm).

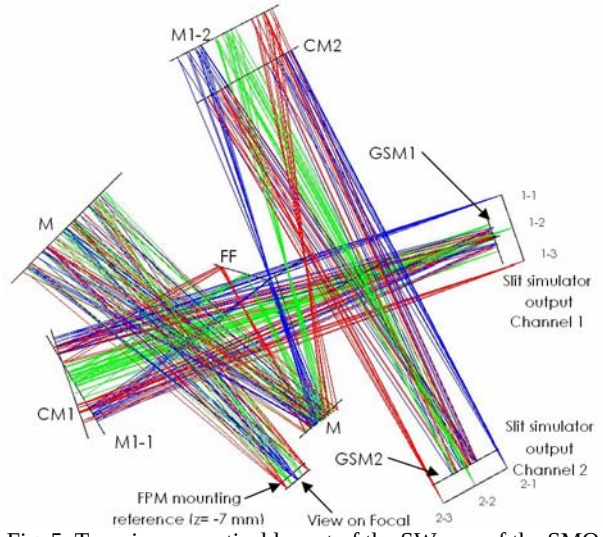

Fig. 5. Top view on optical layout of the SW arm of the SMO with spot number assignments and their corresponding locations in the focal plane.

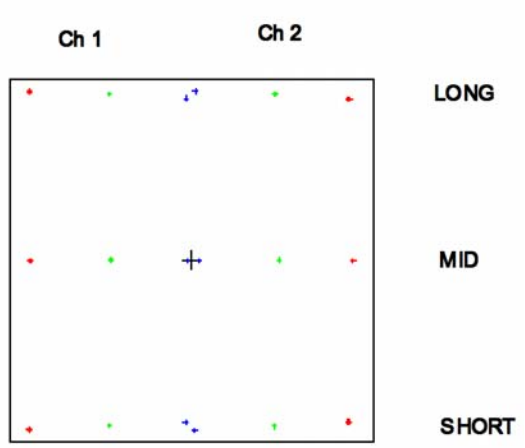

Fig. 6. Footprint in the focal plane of the SW arm; size 28 x 28 mm.

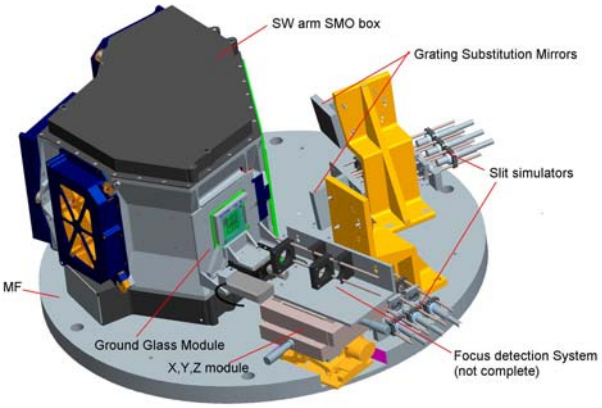

Fig. 7. Measurement setup of the OGSE to determine position of best focus of the SW arm of the SMO

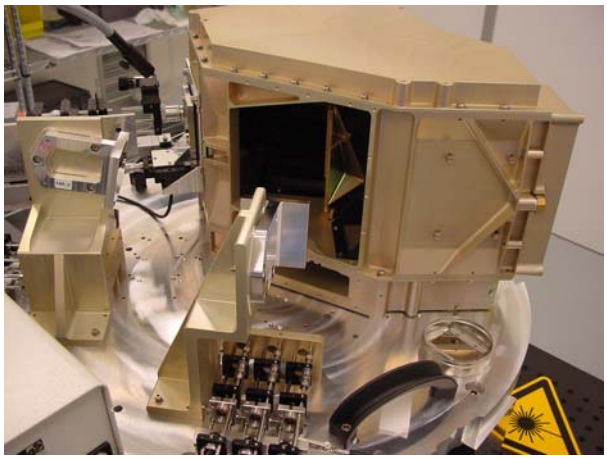

Fig. 8. Measurement setup of the OGSE to determine position of best focus of the SW arm of the SMO

For both SW and LW arm, each of the 36 image spots (2 arms, 2 channels, 3 GSM positions and 3 slit positions) on 11 recorded images are investigated to determine the position of best focus. An example of (part) of such a sequence is shown in Figure 9. Best focus is determined automatically using image processing software.

Fig. 9. Example of a sequence of focus spots. Best focus was found between step 4 and 5. The box size is 0.145 x 0.145mm.

Scripts were developed to determine a number of characteristics of the imaged spots, such as rms spot radius (with and without weighing by intensity) and ellipticity.

After analyzing the characteristics, the best method appeared to be to determine the rms spot radius by only using pixels with intensities higher than the average background + 8 times the sigma of the background level. To find best focus, the rms spot radius in pixels vs. focus position is fitted by a parabola, the minimum of which indicates best focus. An example of such a measurement, the same series as used for Figure 9, is given in Figure 10. For this example the resulting best focus is located at step = 4.43.

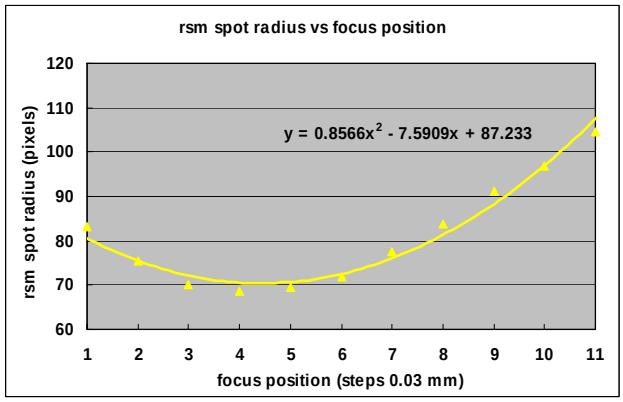

Fig. 10. Spot radius vs. focus position with fitted parabola

The step number of best focus is converted to an 'absolute' Z-position distance with respect to the mounting flange of the Focal Plane Module. Finally the Z-position is corrected for position and tilt of the ground glass.

Error analysis shows that the location of the minimum for a well defined parabola as shown in the example above may be determined with an accuracy of ±0.4 steps or ±0.012 mm. The total accuracy of the measured position of best focus also depends on the individual errors caused by positioning of modules, thickness of shims, etc. The estimated total error of position of best focus is ±0.028 mm (P-V).

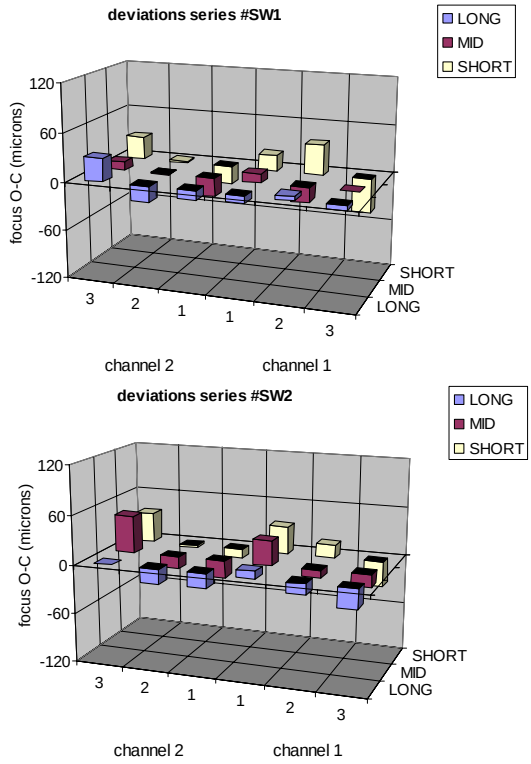

Fig. 11. Deviations (measured minus model) in focus positions for individual image spots (in microns) before TVC (#SW1) and after TVC (#SW2).

The maximum focus error depends on the method of shimming: no shimming at all, shimming of the FPM only (channels are balanced around best focus) and shimming of FPM and M1 individually. Even without shims all series pass the focus criteria, hence shims are not applied.

Table 1. No shims: Focus errors, error budget and pass/fail.

ID	worst channel offset (mm)	Focal pos. errors (mm)	worst focus error (mm)	error budget (mm)	pass or fail?
series SW#1	**0.023**	**±0.028**	**±0.051**	**±0.095**	**pass**
series LW#1	**0.042**	**±0.028**	**±0.070**	**±0.095**	**pass**
series SW#2	**0.023**	**±0.028**	**±0.051**	**±0.095**	**pass**
series LW#2	**0.028**	**±0.028**	**±0.056**	**±0.095**	**pass**

The effect of TVC is determined best by comparing the position of the focal plane for the two series. A total error for the determination of focus position of ±0.019 mm P V is to be expected. This confirms the stability of both SMO FM and OGSE as well as the repeatability and accuracy of the measurements.

4.2 IMAGE QUALITY

The focus spots are collimated by a doublet to provide a pupil onto the lenslet array of the Shack-Hartmann wavefront sensor.

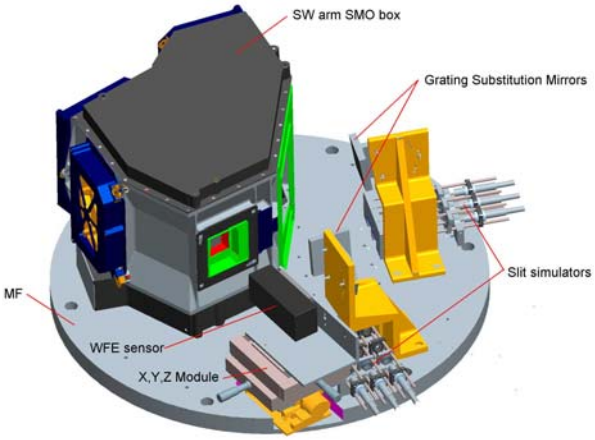

Fig. 12. Measurement setup of the OGSE to determine image quality of the SW arm of the SMO

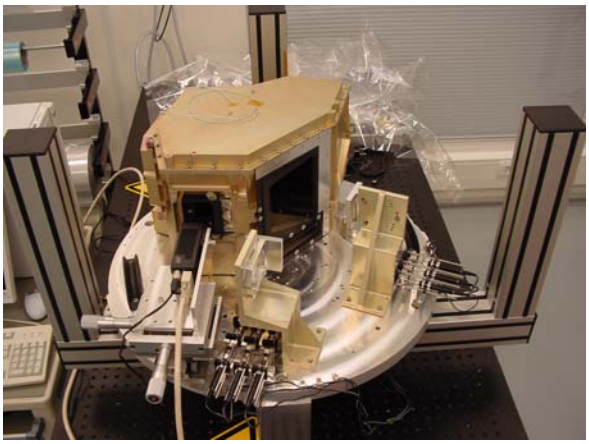

Fig. 13. Actual measuring setup in the clean room with gold-coloured SMO box in the background, SSM and GSM of channel 1 to the right, SSM and GSM of channel 2 in the foreground, and to the left the X,Y,Z-module with black SHSLab Wavefront Sensor System.

To determine the image quality of an image spot, the Wavefront Sensor System (WSS) is manipulated in X, Y and tilt to centre the pupil on the lenslet array of the Shack-Hartmann (S-H) wavefront sensor. The light level is adjusted to give a stable read-out for most of the aperture. In practice the pupil size had to be reduced to about 3.7 mm equivalent to a NA of 0.024. Focussing of the WSS is performed by moving the assembly in the Z-direction and minimizing the Zernike power/focus term Z4 for the image spot being measured. Figure 14 and 15 show an example of the display of the measured, corrected and fitted wavefront errors expressed in P-V and RMS waves (wavelength 670 nm).

The measured wavefront is the wavefront reconstructed directly from the S-H measurements. The corrected wavefront is the wavefront after corrections for piston, tilt and power (Zernike terms Z1 through Z4) as these Wave Front Errors (WFE) do not degrade the image quality in the best focus. The fitted wavefront is the wavefront fitted to Zernike terms Z5 - Z16.

To verify the stability, the measurements are done 3 times and the results are averaged. The measuring procedure is executed for all 36 image spots of the SW and LW arm: 4 channels, 3 GSM positions and 3 slit positions.

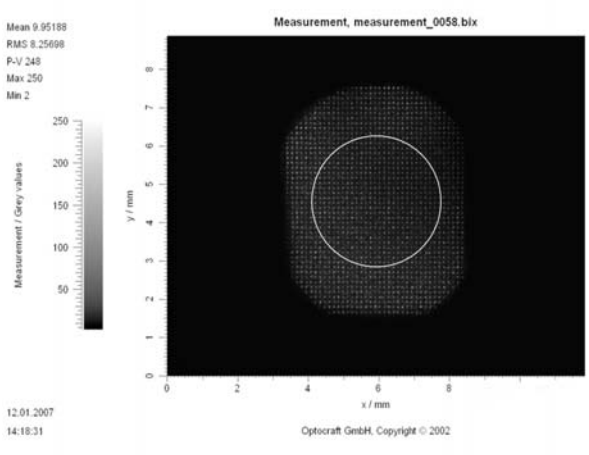

Fig. 14. Shack-Hartmann spots for a NA = 0.040; to avoid vignetting and to improve measuring stability only the image spots within the white circle corresponding with NA = 0.024 will be used.

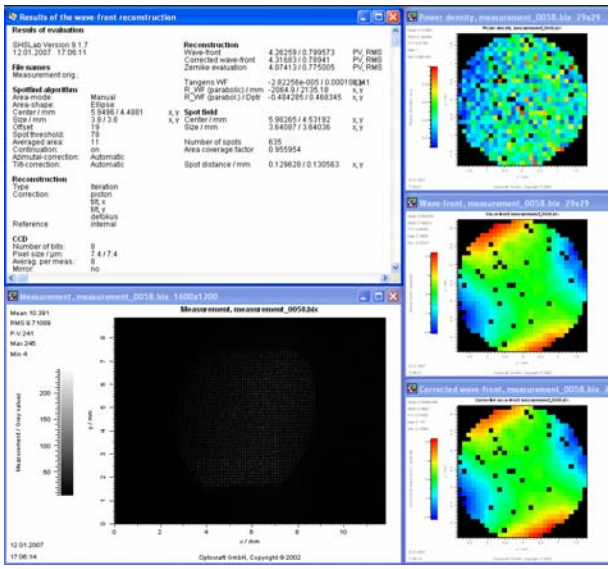

Fig. 15. Example of wavefront measurement of an image spot showing a corrected RMS WFE of 0.789 lambda (wavelength 670 nm). The wavefront suffers from astigmatism.

The SMO as measured in the clean room deviate from the JWST operational configuration as to be used in space by a different pupil (round pupil versus hexagonal mosaic mirror) and a tilted mirror (GSM) in stead of a grating. To be able to compare the measurement results with the 340 nm RMS WFE requirements for the spots, the measured WFEs measured have to be 'extrapolated' to the operational configuration.

In most channels the image quality as calculated with the ZEMAX simulation of the JWST operational model is different from the image quality of the measurement setup. This is caused mainly by the change in pupil size, but also by the anamorphic magnification due to the gratings. In channel 1A the JWST pupil is slightly smaller than NA=0.024, but in all other channels the JWST pupil is considerably larger. See also the footprints in Appendix A.

The final image quality on the detector will also be affected by the Z-position of the detector with respect to the focal plane. Measurements of the best focus show that the position of the focal plane array may differ from its nominal position by less than ±0.07 mm. This is equivalent to an induced wavefront error of 70 nm. This error is also added RSS to the wavefront.

At last a correction has to be applied for normalization of the WFEs to a wavelength of 8 microns. According to the requirements this normalization, multiplication by 8.0/wavelength, is allowed only for wavelengths longer than 8 microns.

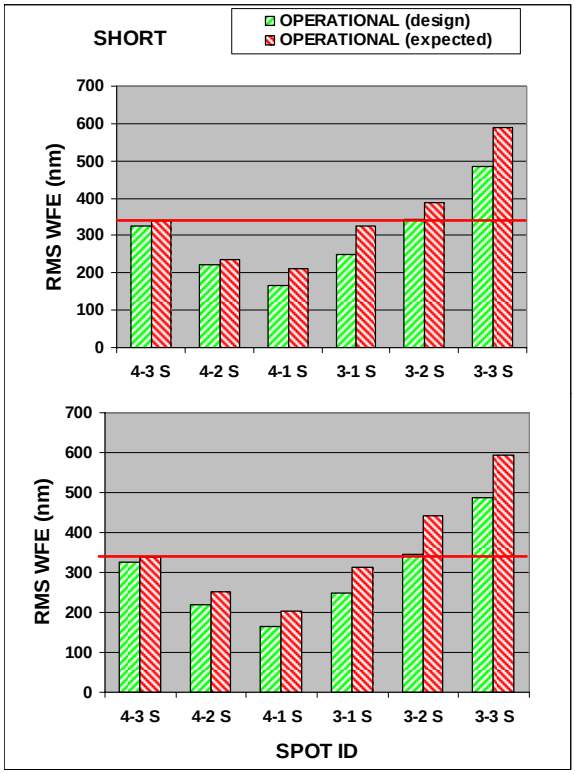

Fig. 16. WFEs as designed and extrapolated from the measurements of the LW arm of the operational JWST configuration. WFE before TVC (top) and after TVC (bottom) are shown. The horizontal line is the budget of 340 nm.

The resulting total WFEs are considered to be representative for the measurements as if they were done with a full operational configuration of the SMO with the correct JWST pupil and gratings. For visual inspection and comparison, the WFEs from design and extrapolated from the measurements are displayed figure 16.

A direct comparison of image spots WFEs for the design and as measured show that for NA=0.024 the measured values are always worse than designed (340nm). The best image spots have WFEs of about 200 nm RMS and the worst have a WFE of about 700 nm RMS. The most prominent aberration contributing to the WFE is this astigmatism. Several tests have been carried to investigate the source of astigmatism, but no firm conclusions could be drawn here. Sensitivity analysis shows that the image quality is most sensitive to surface form errors of M3. But interferometric measurements of M3 mirror mounted in the SMO SW arm could explain only 40% of the astigmatism measured.

The differences found are relatively small with respect to the measured WFE and show no systematic pattern over the detector. As in addition TVC showed no significant change for focus and image positions, the differences are considered not to represent real changes in the mirror surfaces and/or mechanical structure of the SMO.

4.3 IMAGE POSITION

The focus spots are imaged onto the mounted SPM grid. Superimposed images of grid and focus spots are projected by a telecentric objective onto a detector as is shown in figures 17, 18 and 19.

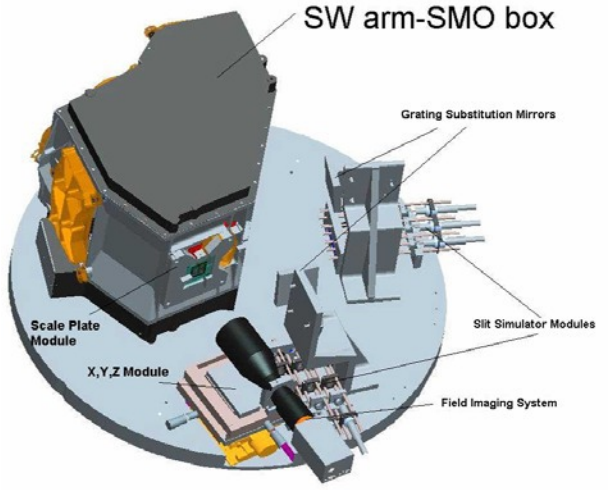

Fig. 17. Measurement setup of the OGSE to determine position of the SW arm of the SMO.

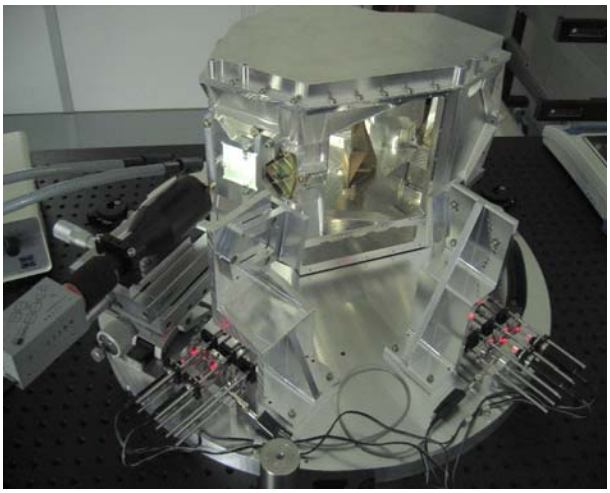

Fig. 18. Actual measuring setup in the clean room with SMO box, SSM and GSM of channel 1 to the right and SSM and GSM of channel 2 to the left. Further to the left is the X,Y,Z-module with black telecentric objective and image digitizer.

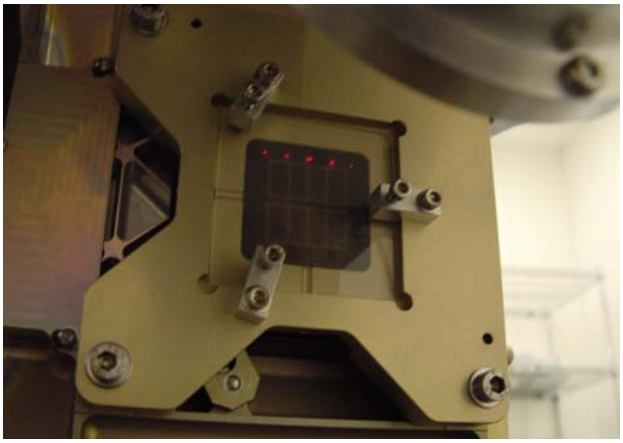

Fig. 19. Details of the Scale Plate Module with its mounted scale plate. All lasers of channel 1 and 2 are switched on with both GSMs in the short wave position

For each of the three GSM positions two images are taken. One image with a short exposure time to register an image with the 6 spots and another image with a long exposure time to record the Scale Plate Module (SPM) grid. The grid on the SPM is illuminated by a flexible fibre optics light guide with the light level adjusted for best contrast. Figure 20 shows an example of such images.

Repeated measurements showed that the accuracy of one measurement of spot or line crossing of a Grid Reference Point (GRP) is ±0.012 mm. By using the co-ordinates and measurements of the GRPs, the position of the spot is transformed to the co-ordinate system of the GRPs. On average the positions of spot and GRP were determined in three exposures, so the measurement error in the position of the spot = ±0.010 mm or ±0.4 MIRI Focal Plane Module (FPM) pixels of 0.025 mm.

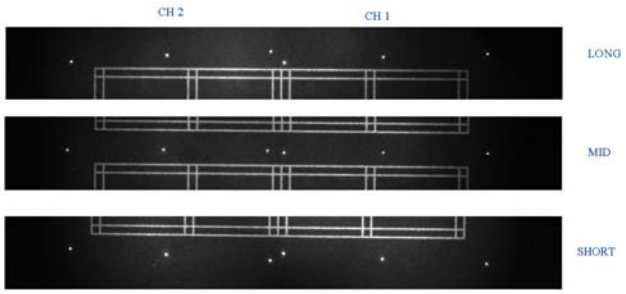

Fig. 20. Combination of three images with spots and SPM grid for channel 1 and 2 with GSM set to long, mid and short wavelength.

The results of the series LW#1 and series LW#2 measurements, and the effects caused by vibration tests and Thermal Vacuum Cycling, are shown in Table 9. For X and Y the deviations from the predicted positions is given (expressed in pixels of 0.025 mm). All measured positions are stable to 1 or 2 pixels.

Table 2. Stability of image position errors of channels after integration, after vibration testing and after TVC. Unit = pixel.

SMO status	channel	worst deviation X (pixels)	Worst deviation Y (pixels)
after integration	1	7	3
after vibration		7	3
after TVC		7	3
after integration	2	5	4
after vibration		7	3
after TVC		7	2
after integration	3	10	5
after vibration		9	6
after TVC		10	7
after integration	4	7	3
after vibration		7	3
after TVC		7	3

6. CONCLUSIONS

This paper and the SMO project show that accurate optical performance is achievable without actively controlling alignment. In this way a huge reduction in assembly and test time/cost is achieved. Maybe more important, a much more stable instrument is provided, without risks of wandering adjustments.

When the fundamental alignment philosophy is based on manufacturing precision only (i.e. 'no adjustment' philosophy) extensive alignment budget monitoring during the whole instrument development is necessary. This budget predicts the correct performance of the SMO as shown in this paper. Eventually numerous tests and measurements took place on the SMO flight model to verify the correct performance. These measurements showed not only that the SMO functions as expected, but also that – for the SMO – the chosen 'no adjustment' philosophy is the optimum design approach (i.e. the balance of instrument performance and project programmatics).

Proper alignment budget monitoring requires extensive knowledge of both the optical and mechanical design and their interaction by means of analyses and error budgeting. With this detailed knowledge it is even possible to redistribute the error over the optical components during development and production. In this way high accuracy vs. costs can be balanced even more.

REFERENCES

1. Yvon, R., et al., "VISIR: a mid-infrared imager and spectrometer for the VLT", Proceedigns of SPIE, Vol. 2475, p. 286-295, Infrared Detectors and Instrumentation for Astronomy, June 1995.

2. Kroes, G. et al., MIRI-JWST spectrometer main optics opto-mechanical design and prototyping, Proceedings of SPIE - Volume 5877 Optomechanics 2005, pp. 244-255, Augustus 2005.

3. Kruizinga B., et.al., MIRI Spectrometer Optical Design, Proceedings of the 5th international conference on space optics ICSO 2004, Toulouse, France, 30 March - 2 Apr., 2004.

4. Wright G., Dishoeck E. van, et.al., The JWST MIRI instrument concept, Proceedings of SPIE - Volume 5487 Optical, Infrared, and Millimeter Space Telescopes, pp. 653-663, Glasgow (UK), October 2004.

5. Wells, M., et al., The MIRI Medium Resolution Spectrometer for the James Webb Space Telescope, Proceedings of the SPIE, Volume 6265, pp. 626514 (2006).

6. Wells, M., et al., The MIRI spectrometer IFUs in a cryogenic space environment, New Astronomy Reviews, Volume 50, Issue 4-5, p. 290-293, 2006

7. Meijers, M., et al, MIRI-JWST Spectrometer Main Optics Qualification & Verification Philosophy, Proceedings of SPIE, to be published, San Diego, 2007.